PHYSICAL REVIEW B VOLUME 15, NUMBER 1 1 JANUARY 1977

Interpretation of the magnetic properties of pseudobinary $Sm_2(Co, M)_{17}$ compounds. I. Magnetocrystalline anisotropy

R. S. Perkins and S. Strässler
Brown Boveri Research Center, CH-5401 Baden, Switzerland
(Received 13 July 1976)

The magnetocrystalline anisotropy of $Sm_2(Co, M)_{17}$ and $Y_2(Co, M)_{17}$ compounds, with M = Fe, Mn, or Cr, has been measured as a function of composition and temperature. The data yield the itinerant-electron and crystal-field contributions to the anisotropy. From the former, the role of band-structure changes is judged to be of equal importance to preferential substitution effects in determining the type and magnitude of the transition-metal sublattice anisotropy. A simplified single-ion crystal-field theory is used to derive the exchange- and crystal-field parameters. The magnitude of their variations cannot be explained by magnetic-moment and lattice-parameter changes alone. Calculations for the structure concerned suggests that in the crystal-field case, charge-transfer effects may be important. However, both changes in the atomic coordinates and in the conduction-electron concentration can also be relevant to both crystal-field and exchange-field concentration dependences.

INTRODUCTION

A sustained interest in the unique hard magnetic properties of transition-metal (TM) rich intermetallic compounds with samarium and other rare-earth (R) elements, has led to the accumulation of a large amount of experimental data concerning their magnetic properties. Of particular interest has been the compound Sm_2Co_{17}.[1] This material exhibits a high magnetization and Curie temperature but severely reduced magneto-crystalline anisotropy, compared to that of $SmCo_5$. Much effort has therefore been devoted to understanding the anisotropy. The large crystal-field contribution has been investigated theoretically.[2-4] The effects of varying electron concentration and rare-earth element are also well documented,[5-16] and an improved understanding of the influence of crystallographic idiosyncrasies of the 2:17 structures has also been obtained.[17-21] A quantitative analysis of the anisotropy of any 2:17 compound is, however, lacking.

Despite attempts with alternative systems,[5] those of samarium exhibit the greatest potential for permanent magnet development.[14,15] For this reason an extensive analysis of three pseudobinary, samarium-based systems has been undertaken; namely, $Sm_2(Co_{1-x}Fe_x)_{17}$, $0 \leq x \leq 0.4$; $Sm_2(Co_{1-x}Mn_x)_{17}$, $0 \leq x \leq 0.25$, and $Sm_2(Co_{1-x}Cr_x)_{17}$, $0 \leq x \leq 0.1$. In addition, the corresponding yttrium-based series were also investigated. The concentration and temperature dependence of the bulk magnetization M_s and the magnetocrystalline anisotropy K, were determined. In both cases the data have been subdivided into their transition-metal and samarium contributions.

This paper is concerned with the anisotropy data. These data permit firstly a qualitative examination of the itinerant-electron contribution. Application of crystal-field theory, however, allows quantitative analysis of the dominant samarium contribution. This yields the variations in the crystal-field and exchange-field parameters due to cobalt substitution. The phenomena which most sensitively influence the anisotropy of these compounds may then be identified.

The transition-metal and samarium magnetic moments are the subject of Paper II. An indication of the changes in the itinerant-electron band structure is obtained. Additionally a calculation is made of the Sm^{3+} ionic moment utilizing the exchange- and crystal-field data derived here.

The investigations yield a closer understanding of the primary magnetic properties of a new class[22] of permanent magnetic materials, which will attain considerable technological importance as a supplement to $SmCo_5$.

EXPERIMENTAL

The pseudobinary alloy series $Sm_2(Co_{1-x}M_x)_{17}$ with M= Fe, Mn, and Cr, and corresponding Y-based compounds, have been investigated. Single-crystal samples were obtained directly from induction-melted charges.[13-15] 99.9% pure Sm and 99.99% pure Co, Fe, Mn, and/or Cr were melted together in a pyrolytic boron nitride crucible. Approximately 8% by weight excess Sm was necessary to maintain the required stoichiometry. This was controlled by wet chemical analysis whilst the TM relationships were assumed to be those when first weighed out. This is only likely to lead to error in the case of manganese. Large grain material from 100-g charges was subsequently homogenized by heat treating at between 1100 and 1200 °C for 3 to 4 days.

The phase constitution of the resulting material was determined by x-ray and metallographic investigations. These showed the solubility limits in the Mn and Cr systems to be approximately $x = 0.25$ and 0.1, respectively. As is already known,[10] the Fe-containing series was fully miscible. The reduced grain size beyond 40-at.% Fe limited the maximum concentration studied to this value. Particularly in the vicinity of the phase boundaries, small undissolved quantities of the corresponding Co-based eutectic persisted.

In all $Sm_2(Co, M)_{17}$ substitution series the $R\bar{3}m$ 2:17 structure modification is observed. Beyond the phase boundary in the Mn compounds both the 6:23 and 1:12 structure types appeared to occur. However, owing to the similarity between all three structures a reliable identification was not obtained. Cr does not appear to form any compound with Sm, and an identification of the phases found beyond the $Sm_2(Co, Cr)_{17}$ limit was not made. In the Y-based compounds, both the $R\bar{3}m$ and $P6_3/mmc$ 2:17 structure modifications were normally observed. This is not uncommon in Y_2Co_{17} type alloys.[13,23]

The measurements of saturation magnetization and anisotropy were carried out with a vibrating sample magnetometer equipped to cover the temperature range $77 \leq T \leq 1000$ K. The analysis of these measurements follows that commonly used.[13] It should be noted that the error incurred in the determination of the K_1 values from the experimental data, owing to the finite exchange field, is only a few percent. The anisotropy energy represents in all cases less than 5% of the exchange energy. In this case Sm and M moments remain essentially parallel at the low fields used.

Single-crystal samples were used, and typically four specimens measured per composition. The crystalline perfection was easily recognizable in the measurements. Specimen alignment was easily achieved to within 2° in a magnetic field, since the anisotropy was always uniaxial in the c axis. None was observable within the basal plane. The rotatable magnet yielded a maximum field of 21 kOe.

RESULTS

Figures 1(a)–1(c) show the composition and temperature dependence of the anisotropy constant, K_1, for $Sm_2(Co, M)_{17}$ with M = Fe, Mn, and Cr, respectively. Figures 2(a) and 2(b) contain these data for the corresponding Y-based compounds. In the Sm alloys K_1 represents the measured anisotropy since the second anisotropy constant $K_2 \ll K_1$. However, in the Y compounds K_2 is appreciable and the appropriate analysis[13] has been carried out to obtain K_1.

Owing to the limited low-temperature range, the curves were extrapolated below 77 K. The error incurred will be commented upon at a later stage. Figures 3(a) and 3(b) contain the values of K_1 at 0 K obtained from the above data. The $Sm_2(Co_{0.85}Mn_{0.15})_{17}$ result was obtained from repeated measurements on two separate preparations. In the case of the $Sm_2(Co, Cr)_{17}$ samples, insufficient concentrations were measured to enable a satisfactory description of the $K_1(x)$ behavior. Also their poor low-temperature data increase the uncertainty of the values shown. However, the trend to higher K_1 does seem genuine. The anisotropy of $Y_2(Co, Cr)_{17}$ samples proved to be very much smaller throughout the temperature range than in the Fe and Mn series. Poor specimen quality prevented an accurate determination of $K_1(x, T)$.

The magnetization data of the above samples are presented separately in Paper II.

THEORETICAL BASIS TO THE ANALYSIS

The contribution to the total anisotropy from the itinerant-electron transition-metal sublattice does not lend itself easily to calculation.[24,25] In contrast the crystal-field contribution is well understood.[2-4]

Existing calculations[2-4] of the crystal-field anisotropy of $SmCo_5$ were based on a single-ion point-charge model. They involve diagonalization of the matrix utilizing the Hamiltonian:

$$\mathcal{H} = \lambda \vec{L} \cdot \vec{S} + \mathcal{H}_c + 2\mu_B \vec{H}_{ex} \cdot \vec{S} \tag{1}$$

of a Sm^{3+} ion experiencing spin-orbit coupling, crystal-field, and exchange-field interactions.

We wish to calculate the stabilization energy, E, and its temperature dependence for a Sm^{3+} ion subjected to a crystalline electric field with an exchange field directed along the crystallographic c axis or within the basal plane. In this case $E(T)$ may be directly compared with $K_1(T)$. The former is defined as

$$E(T) = F(0) - F(90), \tag{2}$$

where

$$F(\phi, T) = -kT \ln \sum_i e^{-E_i(\phi)/kT} \tag{3}$$

is the free energy and $E_i(\phi)$ are the eigenvalues of the matrix

$$\langle JM | \mathcal{H} | J'M' \rangle,$$

ϕ referring to the angle between the exchange field and the c axis.

Following previous arguments,[2-4] attention may

be concentrated on the first of the crystal-field coefficients:

$$\mathcal{H}_c = B_2^0 O_2^0, \tag{4}$$

where the Stevens operator equivalent method yields

$$O_2^0 = 3J_z^2 - J(J+1) \tag{5}$$

and

$$B_2^0 = \alpha_J \langle r^2 \rangle A_2^0 \tag{6}$$

defined in the normal way,[2-4] with

$$A_2^0 = e^2 \sum_k \frac{z_k}{R_k^3} (3\cos^2\theta_k - 1) \tag{7}$$

being the first crystal-field constant, involving summation over the neighboring ions of charge $z_k e$ situated at (R_k, θ_k) with respect to the Sm^{3+} ion and the c axis.

Assuming the exchange field to be sufficiently large to apply first-order perturbation theory in the crystal field, one obtains for the eigenvalues

$$\begin{aligned} E_M(\phi) &= \langle JM | \mathcal{H} | JM \rangle \\ &= B_2^0 3 \{ M^2 \cos^2\phi + \tfrac{1}{2}[J(J+1) - M^2] \sin^2\phi \} \\ &\quad + 2\mu_B (g_J - 1) H_{ex} M \end{aligned} \tag{8}$$

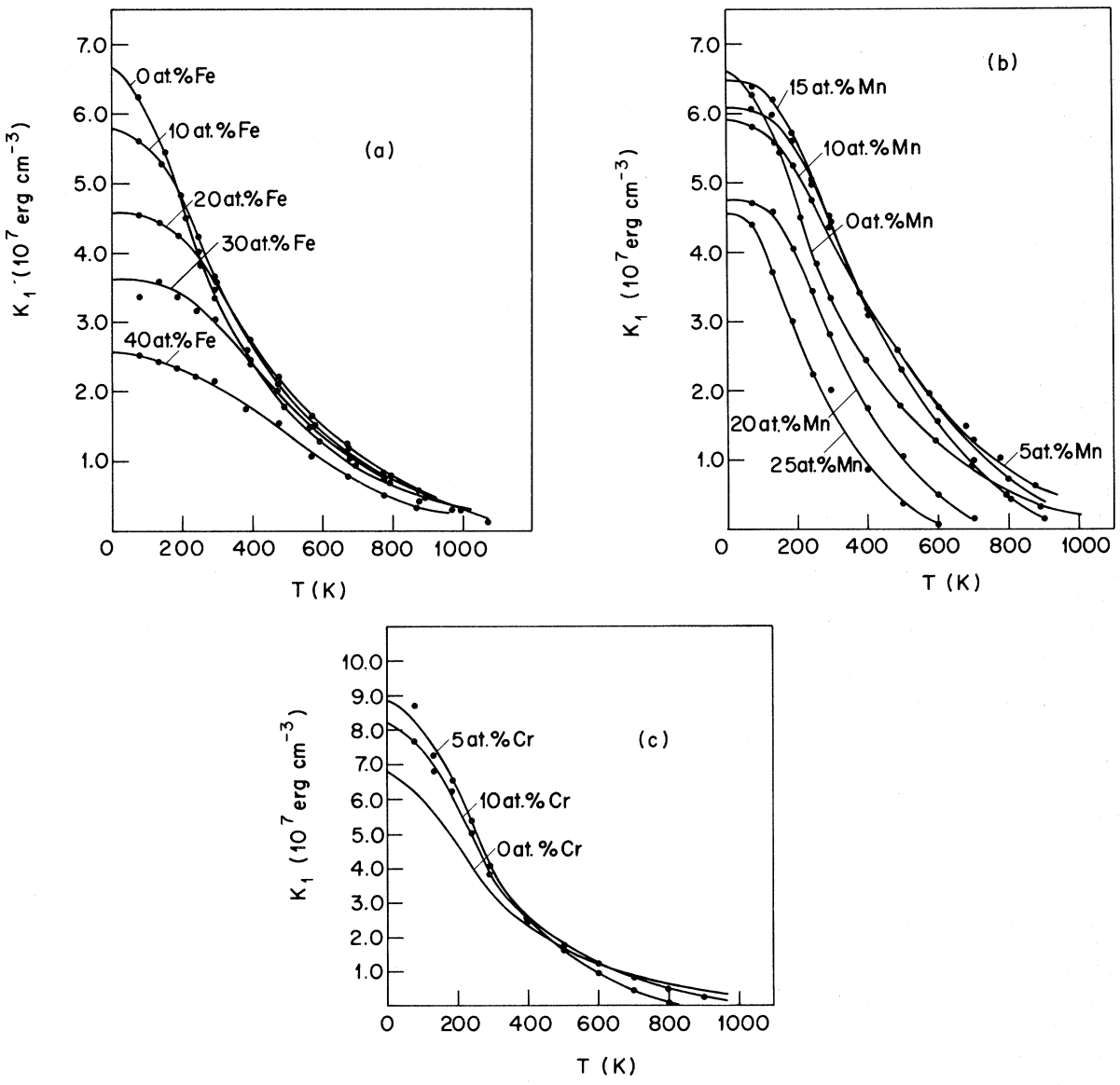

FIG. 1. Temperature and composition dependence of the magnetocrystalline anistropy constant, K_1, in the substitution series $Sm_2(Co_{1-x}M_x)_{17}$ with (a) M = Fe; (b) M = Mn; (c) M = Cr.

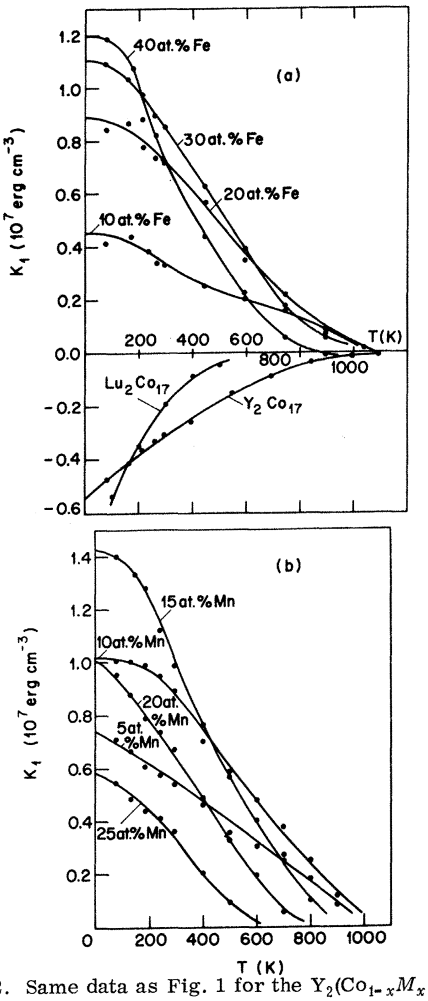

FIG. 2. Same data as Fig. 1 for the $Y_2(Co_{1-x}M_x)_{17}$ compounds with (a) M = Fe; (b) M = Mn.

TABLE I. Comparison between the 0-K stabilization energy calculated from a complete three-level theory (Ref. 3) and the simple theory [Eq. (9)]. All dimensions are in K.

$\langle r^2\rangle A_2^0$	Simple theory	Complete theory	Error
−100	62	75	21%
−200	124	155	25%
−300	186	230	24%

for $J=\frac{5}{2}$; $M=J, J-1, \ldots, -J$. Owing to the relative magnitudes of $\mu_B(g_J-1)H_{ex}$ and B_2^0, typically 30:1, it is the exchange field which essentially determines the temperature dependence of Eq. (2).

The stabilization energy at 0 K becomes

$$E(0) = -B_2^0 3J(J-\tfrac{1}{2}). \tag{9}$$

Hence it is the crystal field which produces the absolute magnitude of the anisotropy.

The results of previous calculations[3] may be used to test the degree of inaccuracy in the above formulas. Table I compares the values of the stabilization energy at 0 K in this way. The more complete theory involved the diagonalization of Eq. (1) for the three lowest Sm^{3+} multiplets, namely, $J=\frac{5}{2}, \frac{7}{2}, \frac{9}{2}$. It is clear that the simple treatment is up to 25% in error, as was also implied in Ref. 3.

On the other hand, the experimental values involve extrapolation from small deviations of the magnetization from the easy direction, whereas the calculation considers only the 0° and 90° positions. A more realistic, but elaborate calculation of $E(0)$ has suggested[3] a consequent overestimation of order 20%. In this eventuality the increased accuracy of the thorough calculation

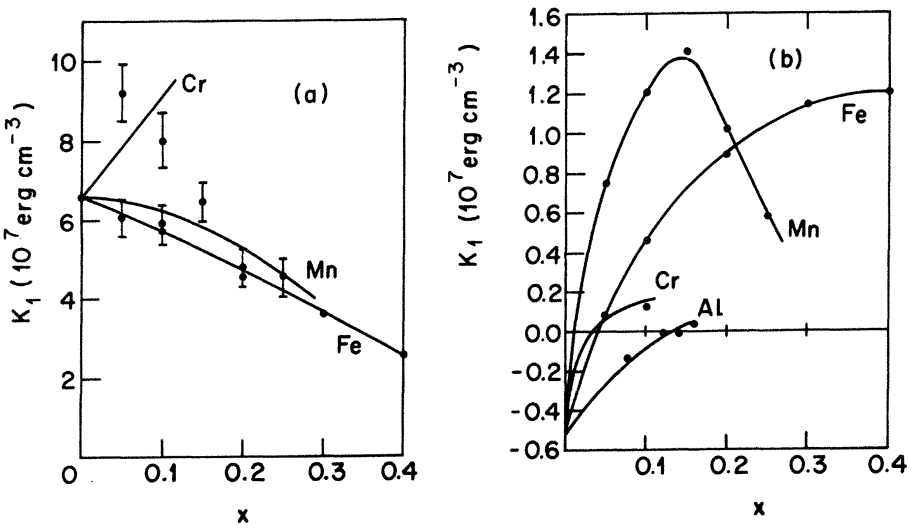

FIG. 3. Anisotropy constant, $K_1(0)$, at absolute zero for the compounds (a) $Sm_2(Co_{1-x}M_x)_{17}$; (b) $Y_2(Co_{1-x}M_x)_{17}$; M = Fe, Mn, Cr, and Al. Al data are taken from Ref. 12.

does not improve the reliability of the analyzed data.

In addition to the above, the temperature dependence derived from Eqs. (2), (3), and (8) proves to be very acceptable. Figure 4 shows a comparison of the normalized $E(T)$ for the same cases as in Table I.

From the above analysis we conclude that we are justified in using the approximation [Eq. (8)] for the eigenvalues of Eq. (1). Its transparency is an obvious advantage in the analysis of the experimental data compared to a computer diagonalization of $\mathcal{H}$ in Eq. (1). The consequences of our approach led to a not unsuccessful attempt at raising the anisotropy of Sm_2Co_{17} and, indeed, formed the incentive for the present study.[15]

DATA REDUCTION

It is assumed that the transition-metal sublattice is essentially the same in both $Sm_2(Co, M)_{17}$ and $Y_2(Co, M)_{17}$. In this case its contribution to the overall anisotropy will be the same in both compounds. By subtraction, the crystal-field contribution in the Sm compounds may therefore be deduced.

The reliability of this approach is difficult to estimate. From the results presented in Paper II, and also for $SmCo_5$,[26] it would appear that the transition-metal part of the band structure is not markedly affected by the presence of a (weakly) magnetic rare-earth ion. However, the anisotropy can be very sensitive to the position of the Fermi level,[25] which would be changed by any loss of Sm $4f$ electrons.[26]

The temperature dependence[11] of the nonmagnetic rare-earth alloy Lu_2Co_{17} is shown in Fig. 2(a). No data have been found for pseudobinary systems. Although $K_1(T)$ is significantly different for the Y and Lu alloys, the difference is not serious when considered against the 10:1 ratio

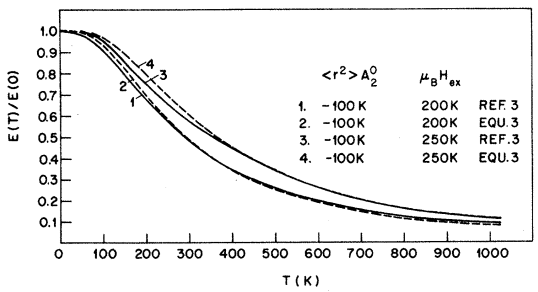

FIG. 4. Comparison of the normalized temperature dependence of the stabilization energy for the complete theoretical treatment of Ref. 3 and the simplified theory presented here. Two values of the exchange field are considered.

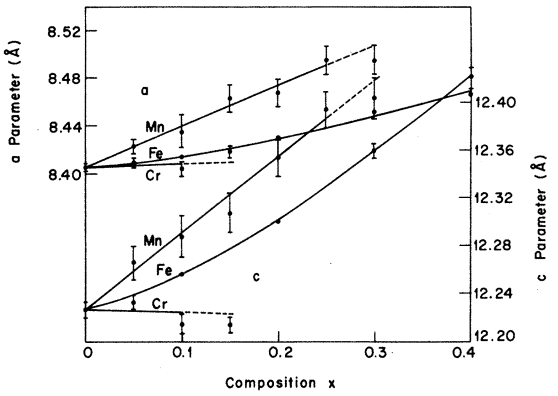

FIG. 5. Lattice-parameter variation within the three $Sm_2(Co_{1-x}M_x)_{17}$ substitution series.

between K_1 for Sm_2Co_{17} and Y_2Co_{17} or Lu_2Co_{17}. The c/a ratio for Y_2Co_{17} is also much closer to that of Sm_2Co_{17} than is Lu_2Co_{17} (1.450, 1.455, and 1.466 respectively).

The densities of $Sm_2(Co, M)_{17}$ may be deduced from the lattice-parameter data of Fig. 5. These are room-temperature data. No temperature dependence was allowed for.

The reduced data of Figs. 1 and 2 are reproduced in Figs. 6 and 7(a)–7(c). Figure 6 indicates the room-temperature variation of the stabilization energy, shown as ΔK_1, whilst Fig. 7 shows the normalized temperature dependence $\Delta K_1(T)/\Delta K_1(0)$. The application of Eqs. (2), (3), (8), and

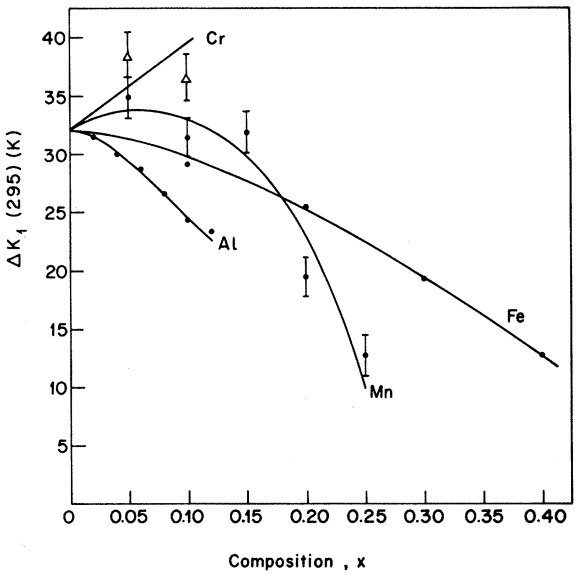

FIG. 6. Comparison of the composition dependence of the measured excess anisotropy energy at room temperature, $\Delta K_1(295)$ for different $Sm_2(Co_{1-x}M_x)_{17}$ compounds; M = Fe, Mn, Cr, and Al.

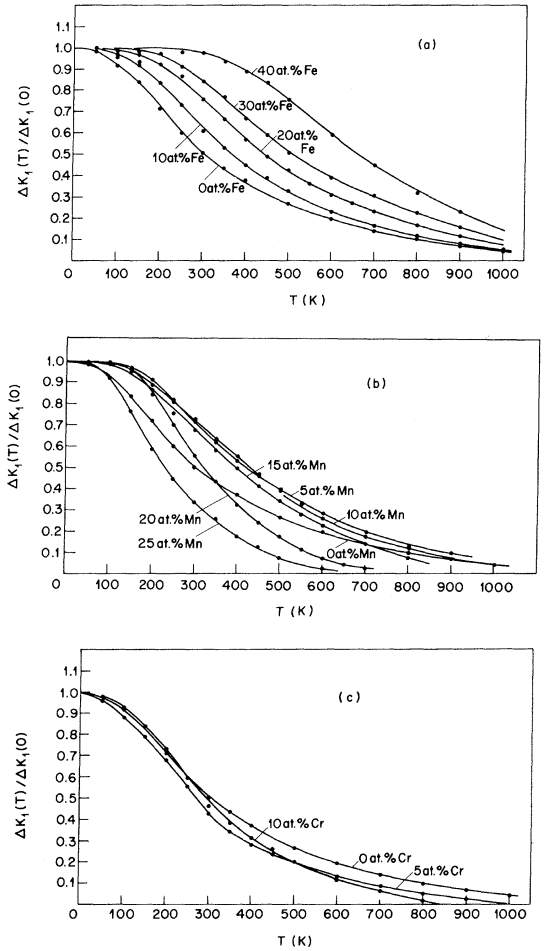

FIG. 7. Normalized temperature dependence of the anisotropy energy $\Delta K_1(T)$ measured in $Sm_2(Co_{1-x}M_x)_{17}$ alloys (a) M = Fe; (b) M = Mn; (c) M = Cr.

(9) allows a determination of the crystal-field and exchange-field parameters $\langle r^2\rangle A_2^0$ and $\mu_B H_{ex}$. From Eq. (8) $\Delta K_1(0)$ is proportional to $\langle r^2\rangle A_2^0$ with

$$\alpha_J 3J(J-\tfrac{1}{2}) = 0.618$$

for all $Sm_2(Co, M)_{17}$; J and the Stevens multiplicative factor α_J being $\frac{5}{2}$ and 0.0412. Figure 8 shows $\langle r^2\rangle A_2^0$ derived in this way for the three alloy series.

Determination of $\mu_B H_{ex}$ involves fitting calculated with experimental normalized temperature dependences. Since H_{ex} is dependent upon the transition-metal moment, it will itself exhibit a temperature dependence. The $H_{ex}(x)$ were therefore assumed to show the same dependence on temperature as the bulk magnetizations presented in Paper II. It should be noted that H_{ex} represents essentially the Sm-TM exchange interaction since

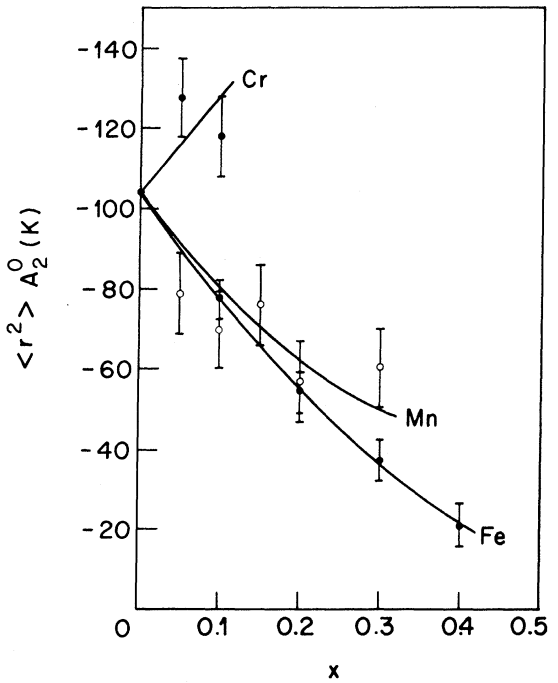

FIG. 8. Crystal-field parameter derived from the data of Fig. 3 with the use of Eq. (9) for the compounds $Sm_2(Co_{1-x}M_x)_{17}$; M = Fe, Mn, and Cr.

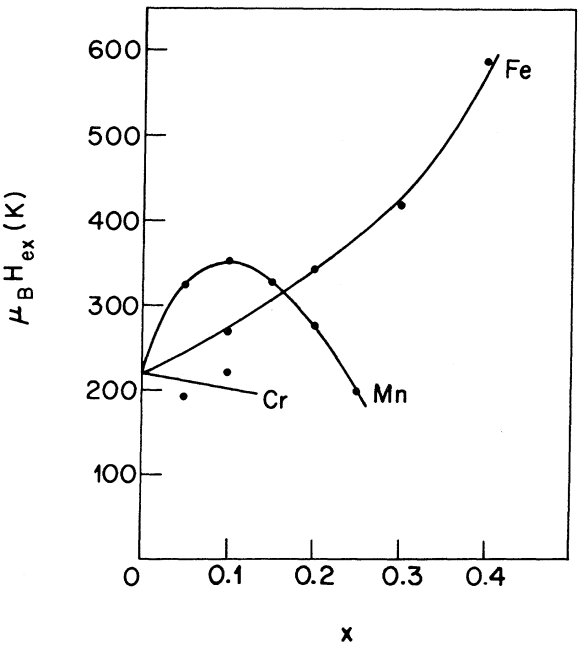

FIG. 9. Exchange-field parameter derived from the data of Fig. 7 with the use of Eqs. (2), (3), and (8) for $Sm_2(Co_{1-x}M_x)_{17}$; M = Fe, Mn, and Cr. $\langle r^2\rangle A_2^0$ of Fig. 8 have been used in Eq. (8).

the Sm-Sm contribution is much weaker.[27]

Least-squares fitting of $E(T)$ with $\Delta K_1(T)$ produced the $\mu_B H_{ex}$ values shown in Fig. 9. The Curie temperatures of Fig. 10 were used in the analyses. An alternative approach, in which $H_{ex}(T)$ follows a Brillouin function, was also applied. The trends shown in Fig. 9 are unchanged although the absolute difference was of order 20 K. However, a Brillouin function is a poor representation of $M_s(T)$.

The above data are summarized in Table II. Additionally the fitted data are reproduced against the experimental data in Figs. 11(a)–11(c). Table II and Fig. 12 also show the corresponding data for $SmCo_5$ using the experimental data of Klein.[28] They are compared with the values from previous analyses, with which they are in good agreement. The deviations between calculated and observed temperature dependences are partially due to the uncertainty resulting from extrapolation. They are, however, also of the type shown in Fig. 4.

DISCUSSION

In view of the two types of anisotropy contained within the experimental data, comments will be made upon both crystal-field and itinerant-electron anisotropy.

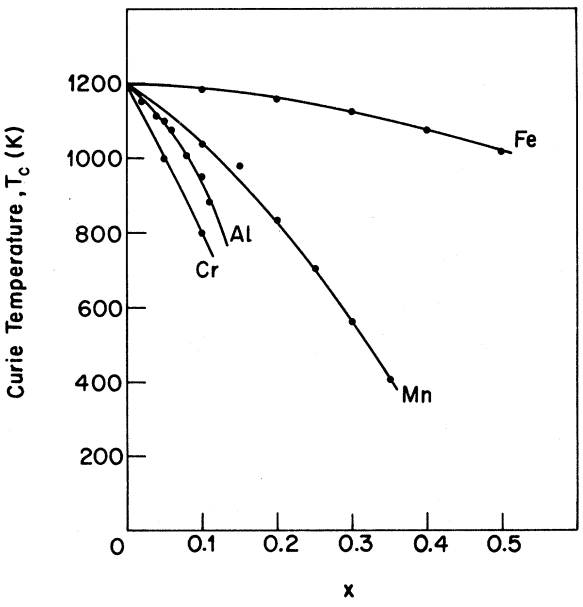

FIG. 10. Curie temperatures of $Sm_2(Co_{1-x}M_x)_{17}$ alloys, with M = Fe, Mn, Cr, and Al. Al data are taken from Ref. 12 and have been normalized to 1200 K for Y_2Co_{17} (from 1182 K).

Transition-metal anisotropy

Previous explanations[18–20] of the composition dependence $K_1(x)$ in $Y_2(Co_{1-x}Fe_x)_{17}$ have concentrated on the possibility of preferential substitution of Co by Fe. The sharp transition to uniaxial anisotropy at 5-at.% Fe is envisaged as a consequence of certain unfavorable interactions having been removed. Whilst this effect may be important, the influence of the electronic band structure upon the anisotropy has previously been ignored.

Band-structure effects

Magnetocrystalline anisotropy in transition metals is due primarily to the removal of degeneracy in the band structure at the Fermi level due to spin-orbit coupling.[24,29] The anisotropy is therefore sensitive to the band structure, as has been shown for Fe, Co, and Ni.[29,30] In particular different structures of the same material lead to different K_1's, as in hcp and fcc Co metal,[29] (-3.4×10^5 erg cm^{-3} and -4.7×10^5 erg cm^{-3} at 500 K) or hcp and double-hcp dilute Co-Fe alloys[31,32] ($+3.7\times10^6$ erg cm^{-3} and -6.9×10^6 erg cm^{-3} for $Co_{0.99}Fe_{0.01}$ at 300 K). It is therefore undoubtedly this band-structure dependence which is responsible for the extraordinarily large K_1 of YCo_5,[28] compared to hcp Co metal (65×10^6 erg cm^{-3} at 0 K). The important ΓA zone[30] of the $SmCo_5$ band structure[33] does not appear to be

TABLE II. Summary of the exchange- and crystal-field parameters derived from the magnetic anisotropy of $Sm_2(Co,M)_{17}$ compounds. The root-mean-square difference is given from the least-squares analysis yielding $\mu_B H_{ex}$. All values given in units K.

M	$\mu_B H_{ex}$	$\langle D^2\rangle^{1/2}$	$\langle r^2\rangle A_2^0$	$\sigma(\langle r^2\rangle A_2^0)$
Sm_2Co_{17}	221	0.015	−104	5
10-at.% Fe	270	0.009	−78	5
20-at.% Fe	344	0.018	−55	5
30-at.% Fe	418	0.022	−38	5
40-at.% Fe	588	0.051	−21	5
5-at.% Mn	325	0.018	−79	10
10-at.% Mn	351	0.014	−70	10
15-at.% Mn	328	0.006	−76	10
20-at.% Mn	276	0.023	−56	10
25-at.% Mn	198	0.027	−60	10
5-at.% Cr	192	0.017	−128	10
10-at.% Cr	222	0.013	−118	10
$SmCo_5$				
Ref. 28	242	0.044	−194	15
Ref. 3	200		−180	
Ref. 2	240		−210	

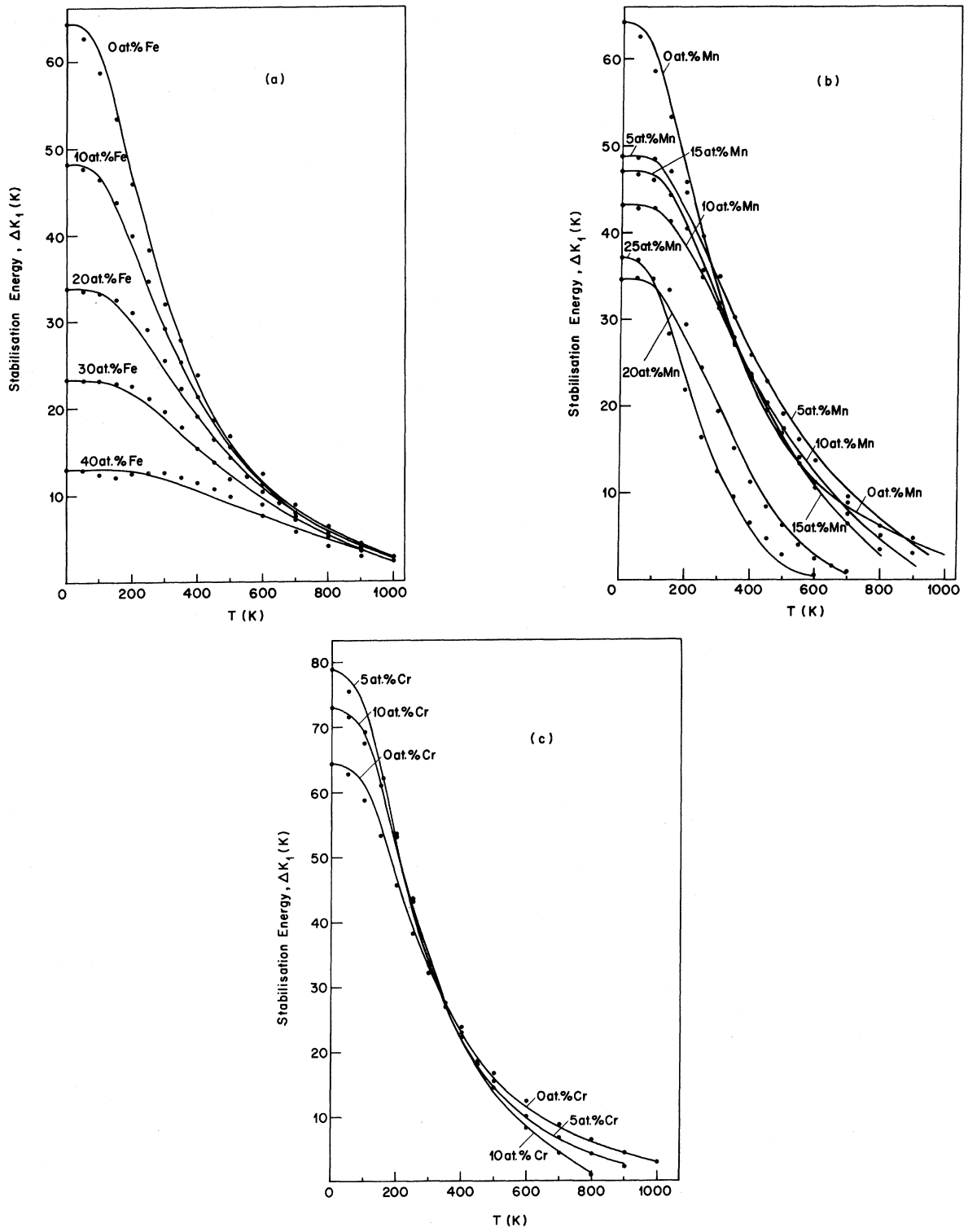

FIG. 11. Results of fitting the stabilization energy calculated from Eqs. (2), (3), (8), and (9) to the experimental data of $Sm_2(Co_{1-x}M_x)_{17}$ for (a) $M=$Fe, (b) $M=$Mn; (c) $M=$Cr. $\langle r^2\rangle A_2^0$, $\mu_B H_{ex}$, and T_C values used are contained in Table II and Fig. 10. Points are experimental values, full lines calculated.

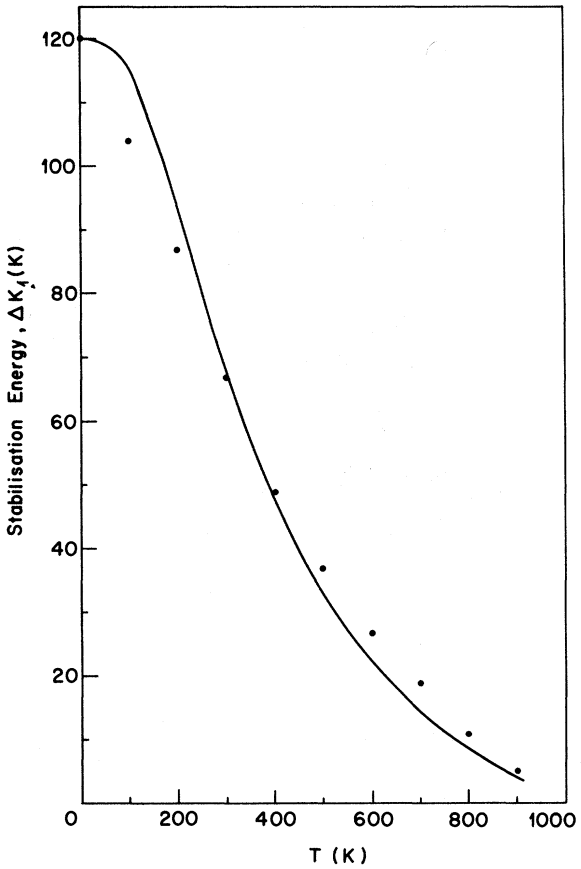

FIG. 12. Similar fit to that of Fig. 11 carried out on the experimental data of Ref. 28 for $SmCo_5$.

markedly different at the Fermi surface to that of hcp Co.[30] However, it is clear from the latter analysis that the contributions from other zones oppose the ΓA value. Were these contributions to support it, then the calculated K_1 value for hcp Co at 0 K would be 59.9×10^6 erg cm^{-3} instead of 8.3×10^6 erg cm^{-3}.

The analogy may be carried a stage further. Y_2Co_{17} exhibits planar anisotropy with $K_1 = -5.4 \times10^6$ erg cm^{-3} at 0 K. Its structure symmetry, $P6_3/mmc$, compared to that of YCo_5, namely $P6/mmm$, shows similar changes to those between double and single hcp CoFe.[31] Loss of basal mirror plane leads to lowering of the sixfold rotation axis symmetry to a 6_3 screw. The consequent changes in the Co-Fe band structure have a dramatic effect upon the anisotropy. The band structures of $SmCo_5$ and hcp Co are not too dissimilar.[33] We speculate therefore that the same mechanism is also responsible for the large anisotropy differences between YCo_5 and Y_2Co_{17} compounds. Furthermore we suggest that the switch to uniaxial anisotropy in $Y_2(Co, Fe)_{17}$ at 5-at.% Fe is equally likely to be caused by band-structure changes resulting from rigid band emptying, as it is to result from preferential substitution. For dilute hcp Co:Fe alloys the addition of Fe also increases K_1 due to the former effect.[30] Ni has the opposite effect. Unfortunately the only data available on $R_2(Co, Ni)_{17}$ compounds are an indication that $Er_2(Co, Ni)_{17}$ switches from uniaxial to planar anisotropy at 10-at.% Ni and in the reverse direction at 40-at.% Ni. This is in contrast to $Er_2(Co, Fe)_{17}$, where the only change occurs at 60-at.% Fe to planar K_1. However, the trend appears to be correct; Fe increasing, Ni decreasing the K_1 of Co at small concentrations.

The case of Co substitution by Mn, Cr, or Al in Y_2Co_{17} [Fig. 3(b)] is not so readily interpreted in terms of band-structure modifications since, as the discussion of Paper II shows, Mn and Cr may exist as virtual bound states. Figure 10 and Ref. 11 show that the Curie temperatures of Fe and Ni containing compounds vary in a similar manner. Substitution by Mn, Cr, or Al leads in contrast to a more rapid decrease of T_C and therefore of the $3d$ band exchange splitting. The consequences for the anisotropy are not easily predictable.

Preferrential substitution effects

The close structural simularity between RCo_5 and R_2Co_{17} suggest the possible role of the TM $6c$ and $18f$ atomic sites in explaining anisotropy differences between the two compounds.[13,17-21] It has been established[18,21] that, even at two widely different Co-Fe composition ratios in $Y_2(Co, Fe)_{17}$, a preferential occupation by Fe of either or both of these sites exists. It would therefore seem plausible that a correlation exists with the anisotropy changes. We have argued against this being the only cause.

In order to correlate preferential substitution with anisotropy it is necessary that the contributions from the atoms at different sites are not equal.[18,21] This has been established[34] for YCo_5, where the orbital contribution to the unpaired electron density at the Co $2(c)$ site appears to be larger than at the $3(g)$ site. Should a similar situation exist in Y_2Co_{17}, then it might be expected that the anisotropy will vary faster in the order Fe, Cr, Mn, Al. This would result from increasing preference of the larger ion for certain sites.[21] As Fig. 3(b) shows, this is the case from Fe to Mn.

A variety of effects are invoked in the following section to explain the magnitude of the variations in the crystal-field anisotropy. We note here

that these may be indirectly influenced by preferential substitution.

Crystal-field anisotropy

The data contained in Figs. 8–10 reproduce the temperature and composition dependence of the crystal-field contribution to the magnetic anisotropy of $Sm_2(Co, M)_{17}$ compounds. An understanding of the factors influencing the crystalline and exchange-field parameters therefore leads to an improved understanding of the anisotropy of a large class of R-TM compounds.

It is appropriate to discuss separately the electrostatic and magnetic interactions.

Crystal-field parameter

From Table II it is clear that the value of A_2^0 is of dominant importance in determining the overall K_1 value of Sm-based alloys. From Eq. (7) it can be seen that A_2^0 is sensitively dependent upon the atomic configuration, the lattice and positional parameters, and the atomic charges and their screening. The effect of these three features upon A_2^0 may be tested with the data of Fig. 8.

The lattice summations in Eq. (8) are most realistically carried out with the use of a screened Coulomb potential of the type

$$V(r) = Z|e| \sum_j \frac{\exp(-k_s|\vec{r} - \vec{R}_j|)}{|\vec{r} - \vec{R}_j|}, \qquad (10)$$

where the jth ionic charge Ze is located at position $\vec{R}_j$. This potential can be conveniently reduced to components of the crystal-field parameters by a spherical harmonic expansion.[35] This yields an approximate screening function for Eq. 7

$$f_2(x) = \tfrac{1}{3}(x^2 + 3x + 3)e^{-x}, \qquad (11)$$

where $x = k_s r$, k_s being the screening parameter and of order 10^{10} m^{-1} for a free-electron gas. We consider further the $R\bar{3}m$ atomic positions for 6c, 18h, and 18f sites from the structure determinations[36] of Pr_2Fe_{17}, and Th_2Co_{17} and Th_2Fe_{17} to be

$$z(R, 6c) = 0.3432 \pm 0.0003;$$

$$z(M, 6c) = 0.0959 \pm 0.0001,$$

$$x(M, 18f) = 0.2858 \pm 0.0005;$$

$$x(M, 18h) = 0.1692 \pm 0.0005,$$

$$z(M, 18h) = 0.4885 \pm 0.0010,$$

where the uncertainty represents deviations between the three compounds. It is notable that the differences between Co- and Fe-based compounds are barely significant.[21]

The source of the anisotropy difference between $SmCo_5$ and Sm_2Co_{17} lies in the different Sm^{3+} environment as well as the different lattice parameter (a is contracted, c expanded in comparison to $SmCo_5$). Evaluating the lattice summation for Sm^{3+} only and $k_s = 1\times10^{10}$ m^{-1} yields the 1:5/2:17 stabilization energy ratio at 0 K of 1.58. This compares with the ratio measured of 1.86. In view of the large error expected in the calculated values, the agreement is fortuitous.

The composition dependences $A_2^0(x)$ cannot be explained in terms of lattice-parameter change alone. Taking again solely Sm^{3+} ions, the structure given above, the lattice parameters of Fig. 5, and $k_s = 1\times10^{10}$ m^{-1}, some $\langle r^2\rangle A_2^0$ values of the three series are given in Table III. It is clear that the measured variations are much larger than those due to a, c changes. Within a 2:17 series the errors arising from the derivation of the $\langle r^2\rangle A_2^0$ values from the measured ΔK should be small. It therefore seems necessary to seek

TABLE III. Comparison between measured and calculated changes of $\langle r^2\rangle A_2^0$. The latter refer to either summation over Sm^{3+} ions, or over both Sm^{3+} ions and M atoms carrying a constant charge Z_M; in this case $+0.2e$. If Z_M is allowed to vary, then the values shown are required to account for the measured A_2^0 changes. The influence of screening-parameter changes is also shown.

at.% M	k_s (10^{10} m^{-1})	$\langle r^2\rangle A_2^0$(K) Measured	Sm^{3+}	$Sm^{3+} + M^{0.2+}$	Z_M
Sm_2Co_{17}	1.2	−104	−163	···	0
Sm_2Co_{17}	1.0	−104	−104	···	0
Sm_2Co_{17}	0.8	−104	−71	···	0
20-at.% Fe	1.0	−55	−98	−96	+0.26
40-at.% Fe	1.0	−21	−93	−89	+0.44
10-at.% Mn	1.0	−70	−99	−98	+0.18
20-at.% Mn	1.0	−56	−96	−94	+0.25
5-at.% Cr	1.0	−128	−103	−104	−0.15

other causes for the faster decreases in $E(0)$. However, the weaknesses of point-charge calculations should not be ignored.

The sensitivity of A_2^0 to the precise atomic coordinates used suggests that the observed $A_2^0(x)$ result from atomic position dependence upon the Co:M ratio. However, the structure changes observed[21] in $Y_2(Co_{0.31}Fe_{0.69})_{19.2}$, which need not be typical of the Sm-based compounds, were found to in fact decrease the composition dependence of A_2^0.

Changes in the screening parameter due to variations in the conduction-electron concentration[37] are also possible. Table III shows the dependence of A_2^0 upon k_s for Sm_2Co_{17}. A progressive decrease in the conduction-electron concentration, and therefore of k_s, accelerates the reduction in $A_2^0(x)$. The changes necessary appear, however, to be unreasonably large.

The most likely remaining cause of the $A_2^0(x)$ dependence is that the TM atom carries a charge. For Sm_2Co_{17} the closest Sm-Co separation is 27% smaller than the closest Sm-Sm distance. From Eq. (7) it is then clear that only a small Co charge would be necessary to substantially alter the lattice summation. Table III shows the values of the hypothetical TM charge required to yield the measured $A_2^0(x)$. These were calculated in a similar manner to that above, where only the Sm^{3+} were assumed. The $Z_m(x)$ values correspond to approximately $+1.2e$/Fe and $+1.5e$/Mn. Various structure modifications were subsequently allowed in order to test this influence on $Z_m(x)$. Whilst the absolute values changed considerably, the dependence was always of the same type; namely, positive increasing for Fe and Mn but negative for Cr. The increased charge transfer between Co:Fe and Co:Mn is consistent with the electronegativity differences of these elements.[38] The existence of a TM charge in RCo_5 compounds has recently been suggested by x-ray spectroscopy.[39]

In summary, the drop in K from $SmCo_5$ to Sm_2Co_{17} is explainable in terms of the simultaneous structural change. The dependence $K_1(x)$ at 0 K in the three alloy series is, in contrast, only partially due to this effect. An explanation of the magnitude of $A_2^0(x)$ requires atomic coordinate variations, screening parameter changes, and/or the presence and variation of a TM atom charge.

Exchange-field parameter

The mechanism responsible for the R-TM exchange field is more likely to be a Ruderman-Kittel-Kasuya-Yosida-type coupling of $3d$ and $4f$ wave functions, than direct $3d$-$4f$ mixing.[27] This indirect exchange may be propagated by s, p, and d conduction states. The exchange energy has been expressed[40] as

$$E_{ex} = \sum_{\nu\nu'} I_1(R_{\nu\nu'}) \vec{S}_\nu \cdot (g-1)\vec{J}_{\nu'}, \tag{12}$$

where

$$I_1(r) = (4me^2/7\pi^3\hbar^2)(B_{00}^3 + \tfrac{9}{5}B_{11}^2 + \tfrac{4}{3}B_{11}^4), \tag{13}$$

where g is the Landé factor of the R ion, S_ν and J_ν, the $3d$ and $4f$ moments, the remaining quantities have their normal meaning, and the approximate values[41]

$$B_{00}^3 = 0.49\langle r^2\rangle \pi k_F^4 J_{sd} F_1(2k_F R), \tag{14}$$

$$B_{11}^2 = 0.10\langle r^2\rangle \pi k_F^6 J_{sd} F_2(2k_F R), \tag{15}$$

$$B_{11}^4 = 0.65 B_{11}^2 \tag{16}$$

contain the Fermi wave vector, k_F, the sd exchange integral, J_{sd}, the mean square $4f$ radius, and Ruderman-Kittel-Kasuya-Yosida-type functions

$$F_1(X) = (X\cos X - \sin X)/X^4 \tag{17}$$

$$F_2(X) = (-X^3\cos X + 7X^2\sin X + 18X\cos X - 18\sin X)/X^6 \tag{18}$$

appropriate to s- and p-type states. Figure 13 shows the dependence of F_1 and F_2 for Sm_2Co_{17} upon k_F. Also shown is $\mu_B H_{ex}/J_{sd}S$. This quantity does not depend sensitively upon the lattice parameter, as also was the case for A_2^0. The $\mu_B H_{ex}(x)$ of Fig. 9 should therefore be explained in terms of TM atom moment, sd exchange integral, and k_F variations with M concentration.

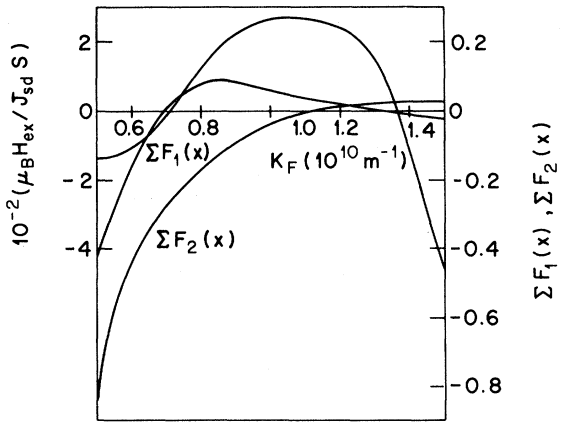

FIG. 13. Summations of the functions $F_1(X)$ and $F_2(X)$ in Eqs. (12)–(18) carried out for Sm_2Co_{17}. Value of Eq. (12), given as the exchange field per unit s-d exchange integral and transition atom spin, $\mu_B H_{ex}/J_{sd}S$, is also shown.

Allowing for the TM moment changes given in Paper II, there still remains an increase of 200% and 150% in the Fe and Mn, $Sm_2(Co, M)_{17}$ series, respectively. Little is known of the values J_{sd} might have in R-TM compounds. The Curie temperatures of Figure 10 indicate only that the dominant direct d-d exchange decreases. Also no reversal of the Sm spin moment with respect to the TM moment occurs (see Paper II).

If the s-d exchange is positive, as suggested for TM based binary alloys,[42] then antiferromagnetic $3d$-$4f$ coupling (see Paper II) demands that the negative portion of Fig. 13 applies. The relationship between k_F and the conduction-electron concentration is not easily established. However, on a free-electron model and in view of the expected 4s-band occupancy and Sm ionicity, the low-k_F region of Fig. 13 is more appropriate. In the absence of data on $J_{sd}(x)$, we remark that a decrease in the conduction-electron concentration could explain the observed $H_{ex}(x)$ in the Fe and Mn series. It should be noted that from Table III, a similar change is also in harmony with the observed $A_2^0(x)$.

CONCLUSIONS

From the analysis of the magnetocrystalline anisotropy of certain $Sm_2(Co, M)_{17}$ compounds we conclude the following. The itinerant-electron anisotropy varies in a similar way for all substitution series. It is argued that the influence of the band structure upon the anisotropy is at least as important as the effects of preferential substitution at certain crystallographic sites. In particular the characteristic switch to uniaxial anisotropy at low substitution levels is considered to result from the former effect.

The magnitude of the crystal-field anisotropy at temperatures of technological interest is determined by both the crystal-field and the exchange-field parameters for the material concerned. Both quantities are sensitively dependent upon the actual atom positions. It has been shown, however, that variations in the conduction-electron concentration may also be responsible for the greater compositional dependence of crystal and exchange fields. Additionally a transition-atom charge, in the crystal-field case, and s-d exchange integral changes, in the exchange-field case, are possible explanations. These effects may, however, be indirectly influenced by preferential TM substitution. Lack of data prevents further evaluations of these effects.

It has been tacitly assumed in this paper that a point-charge model of the crystal-field interactions is sufficiently accurate to justify seeking explanations for the composition dependences of the parameters derived by it. The model is known to be unsatisfactory in many respects. We nevertheless believe that the analysis given here provides a useful indication of the influence of various quite general phenomena upon the anisotropy of a group of technologically important materials.

ACKNOWLEDGMENTS

The authors wish to acknowledge the advice and encouragement of Dr. A. Menth. They would also in particular like to recognize the considerable development activity of Dr. H. Nagel, whose efforts formed the justification and impetus for such an interesting problem. The assistance of Mr. W. Studer in the experimental investigation is also gratefully acknowledged.

[1]K. J. Strnat, IEEE Trans. Magn. MAG-8, 511 (1972).
[2]J. E. Greedan and V. U. S. Rao, J. Solid State Chem. 6, 387 (1973); S. G. Sankar, V. U. S. Rao, E. Segal, W. E. Wallace, W. G. D. Frederick, and H. J. Garrett, Phys. Rev. B 11, 435 (1975).
[3]K. H. J. Buschow, A. M. van Diepen, and H. W. de Wijn, Solid State Commun. 15, 903 (1974).
[4]Yu. P. Irkhin, E. I. Zabolotskii, E. V. Rozenfel'd, and V. P. Karpenko, Fiz. Tverd. Tela 15, 2963 (1973) [Sov. Phys.-Solid State 15, 1976 (1974)]; V. P. Karpenko, Fiz. Tverd. Tela 15, 3714 (1973) [Sov. Phys.-Solid State 15, 2478 (1974)]; Yu. P. Irkhin and E. V. Rozenfel'd, Fiz. Tverd. Tela 16, 485 (1974) [Sov. Phys.-Solid State 16, 310 (1974)]; A. A. Kazakov, A. V. Deryagin, N. V. Kudrevatykh, and V. A. Reimer, Fiz. Tverd. Tela 16, 3732 (1974) [Sov. Phys.-Solid State 16, 2429 (1975)].
[5]K. S. V. L. Narasimhan and W. E. Wallace, *Proceedings of the Tenth Rare Earth Research Conference, Carefree, Arizona* (United States Atomic Energy Commission Technical Information Center, Oak Ridge, Tennessee, 1973), p. 282; AIP Conf. Proc. 18, 1248 (1973); J. Solid State Chem. 13, 315 (1975).
[6]K. S. V. L. Narasimhan, W. E. Wallace, R. D. Hutchens, IEEE Trans. Magn. MAG-10, 729 (1974).
[7]K. S. V. L. Narasimhan, W. E. Wallace, R. D. Hutchens, and J. E. Greedan, AIP Conf. Proc. 18, 1212 (1973); *Proceedings of the Eleventh Rare Earth Conference, Traverse City, Michigan* (United States Atomic Energy Commission Technical Information Center, Oak Ridge, Tennessee, 1974), p. 449.
[8]H. J. Schaller, R. S. Craig, and W. E. Wallace, J. Appl. Phys. 43, 3161 (1972).
[9]A. E. Ray and K. J. Strnat, IEEE Trans. Magn. MAG-8, 516 (1972).
[10]H. F. Mildrum, M. S. Hartings, K. J. Strnat, and J. G. Tront, AIP Conf. Proc. 10, 618 (1973).
[11]A. Deryagin, A. Ulyanov, N. Kudrevatykh,

E. Barabanova, Y. Bashkov, A. Andreev, and E. Tarasov, Phys. Status Solidi A 23, K15 (1974); A. V. Deryagin and N. V. Kudrevatykh, *ibid.* A 30, K129 (1975).

[12]M. Hamano, S. Yajima, and H. Umebayashi, IEEE Trans. Magn. MAG-8, 518 (1972); *Proceedings of the Eleventh Rare Earth Conference, Traverse City, Michigan* (United States Atomic Energy Commission Technical Information Center, Oak Ridge, Tennessee, 1974), p. 477; Trans. Jpn. Inst. Met. 15, 273 (1974).

[13]R. S. Perkins and H. Nagel, Physica B 80, 143 (1975).

[14]R. S. Perkins, S. Gaiffi, and A. Menth, IEEE Trans. Magn. MAG-11, 1431 (1975).

[15]R. S. Perkins, S. Strässler, and A. Menth, AIP Conf. Proc. 29, 610 (1976).

[16]A. E. Müller, K. Miura, H. Rodrigues, and I. D'Silva, AIP Conf. Proc. 24, 672 (1974); A. E. Miller, J. F. Shanley, and T. D'Silva, *Proceedings of the Eleventh Rare Earth Conference, Traverse City, Michigan* (United States Atomic Energy Commission Technical Information Center, Oak Ridge, Tennessee, 1974), p. 469.

[17]D. Givord and R. Lemaire, IEEE Trans. Magn. MAG-10, 109 (1974).

[18]J. Deportes, D. Givord, R. Lemaire, H. Nagai, and Y. T. Yang, J. Less-Common Metals 44, 273 (1976).

[19]P. C. M. Gubbens and K. H. J. Buschow, Phys. Status Solidi A 34, 729 (1976); J. B. A. A. Elemans, P. C. M. Gubbens, and K. H. J. Buschow, J. Less-Common Metals 44, 51 (1976).

[20]C. Do-Dinh, P. Johnson, D. Sparlin, and W. J. James, *Proceedings of the Eleventh Rare Conference, Traverse City, Michigan* (United States Atomic Energy Commission Technical Information Center, Oak Ridge, Tennessee, 1974), p. 460.

[21]R. S. Perkins and P. Fischer, Solid State Commun. (to be published).

[22]H. Nagel, AIP Conf. Proc. 29, 603 (1976).

[23]K. H. J. Buschow, J. Less-Common Metals 11, 204 (1966).

[24]E. I. Kondorskii and E. Straube, Zh. Eksp. Teor. Fiz. 63, 356 (1972) [Sov. Phys.-JETP 36, 188 (1973)].

[25]M. I. Darby and E. D. Isaac, IEEE Trans. Magn. MAG-10, 259 (1974).

[26]F. J. Arlinghaus, IEEE Trans. Magn. MAG-10, 726 (1974).

[27]K. H. J. Buschow, Phys. Status Solidi A 7, 199 (1971).

[28]H. P. Klein, A. Menth, and R. S. Perkins, Physica B 80, 153 (1975).

[29]N. Mori, Y Fukuda, and T. Ukai, J. Phys. Soc. Jpn. 37, 1263 (1974).

[30]N. Mori, T. Ukai, and H. Yoshida, J. Phys. Soc. Jpn. 37, 1272 (1974).

[31]T. Wakiyama, AIP Conf. Proc. 10, 921 (1973).

[32]N. Mori, T. Ukai, and S. Kono, J. Phys. Soc. Jpn. 37, 1278 (1974).

[33]The spin-polarized band structure of $SmCo_5$ from Ref. 26 is perhaps more easily compared with similar calculations for hcp Co in: C. M. Singal and T. P. Das, AIP Conf. Proc. 18, 1049 (1973).

[34]J. Deportes, D. Givord, J. Schweitzer, and F. Tasset, Joint Magnetism and Magnetic Materials/Intermag Conference, Pittsburgh, June (1976) (unpublished).

[35]A. H. Millhouse and A. Furrer, Solid State Commun. 15, 1303 (1974).

[36]Q. Johnson, D. H. Wood, G. S. Smith, and A. E. Ray, Acta Crystallogr. B 24, 274 (1963); Q. Johnson, G. S. Smith, and D. H. Wood, *ibid.* B 25, 464 (1969).

[37]Thomas-Fermi statistics yield for the free-electron case a screening parameter $k_s \propto k_F^{1/2}$ or $n^{1/6}$, the Fermi wave vector and free-electron concentration.

[38]A. R. Miedema, J. Phys. F 3, 1803 (1973).

[39]P. R. Sarode and A. R. Chetal, J. Phys. F 6, L163 (1976); A. R. Chetal and P. R. Sarode, *ibid.* F 5, L217 (1975).

[40]A. A. Kazakov, Fiz. Tverd. Tela 17, 2309 (1975) [Sov. Phys.-Solid State 17, 1527 (1975)].

[41]A. A. Kazakov, Fiz. Tverd. Tela 12, 2021 (1970) [Sov. Phys.-Solid State 12, 1605 (1971)].

[42]M. B. Stearns, J. Appl. Phys. 36, 913 (1965).